Preprints of the 21st IFAC World Congress (Virtual)
Berlin, Germany, July 12-17, 2020

Decentralized Optimal Powertrain Control for Connected Hybrid Electric Vehicles in Merging Scenario

Fuguo Xu * **Tielong Shen** * **Jiangyan Zhang** **

* *Department of Engineering and Applied Sciences, Sophia University, Tokyo 102-8554, Japan (e-mail: fuguoxu@sophia.ac.jp, tetu-sin@sophia.ac.jp)*
** *College of Mechanical and Electronic Engineering, Dalian Minzu University, Dalian 116600, China (e-mail: zhangjy@sophia.ac.jp)*

Abstract: This extended abstract mainly deals with the optimal merging problem for connected hybrid electric vehicles (HEVs), a real-time decentralized optimization strategy is proposed to minimize traveling time and energy consumption for HEVs. Both vehicle dynamics and powertrain operation are optimized simultaneously to achieve the global energy efficiency improvement. A case study is conducted in a multi-vehicle-controllable traffic-in-the-loop powertrain platform to verify the effectiveness of proposed decentralized optimization strategy.

Keywords: Connected vehicles, hybrid electric vehicles (HEVs), merging roadways, real-time decentralized optimization.

1. INTRODUCTION

With the fast development of advanced communicated technology, such as 5th generation, it is possible to achieve the communication of vehicle-to-vehicle (V2V) and vehicle-to-infrastructure (V2I). With V2V and V2I, the driving safety and energy efficiency for connected vehicles can be improved further (Guanetti (2018)). On the other hand, HEVs with ability of multi-source to propel vehicle, the energy utilization rate is higher than conversional vehicle by making engine work in high efficiency. However, the powertrain control of HEVs becomes complex, specially when facing with the real-world traffic scenario.

In the merging scenario for vehicles on two lanes to merge at a point, usually the traffic jam happens because of unsuitable speeds of vehicles from two lanes arriving at the merging point (Zhao (2019)). With the connectivity technology, the cooperative control for vehicles in the merging scenario is possible and there are researches focusing on this topic. (Cao (2015)) proposed a real-time cooperative merging path generation algorithm and the actual speed is controlled to track the planning speed. (Ito (2019)) used pseudo-perturbation-based broadcast control to optimize connected vehicles in merging road. Moreover, (Rios-Torres (2017)) and (Xiao (2019)) developed the decentralized cooperative control for vehicles in the merging scenario. However, only vehicle dynamics is taken into account for optimization algorithm design in above optimization algorithms. Since the powertrain in HEVs plays a critical role in energy efficiency improvement, the powertrain operation should also be co-optimized for vehicles in the merging scenario.

⋆ This work was partially supported by the National Natural Science Foundation of China under Grant 61973053

This paper proposed a decentralized cooperative optimization framework for connected HEVs arriving into the merging scenario with co-optimization of powertrain and vehicle dynamics of HEVs. The aim of this cooperative framework is to fast pass through the merging zone with minimization of energy consumption for the total vehicles. Moreover, the traffic congestion can also be reduced at merging point with effective algorithm.

2. PROBLEM FORMULATION

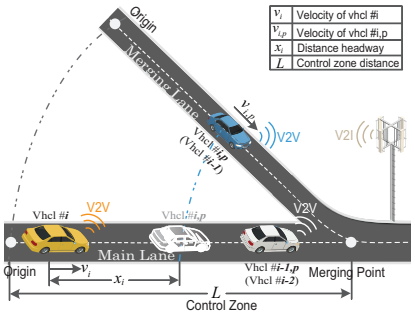

Fig. 1. Structure of merging roads with main lane and merging lane.

The merging problem at the merging point between main lane and merging lane is described in Fig. 1. In this paper, a control zone is defined as a same length L to the merging point for both main lane and merging lane. The vehicles from two lanes can arrive at the control zone randomly. Moreover, it is assumed that no overtaking behavior occurs in the control zone. Based on the principle of First-In-First-Out (FIFO), the preceding vehicle i,p of vehicle i is defined as the last one arriving at the control zone before vehicle i, as is depicted in Fig. 1. The distance x_i between i

and i, p can be determined with V2V communication. For the HEVs within the length L of control zone, the goal is to minimize the travelling time and energy consumption in monetary sense simultaneously. Since the researched vehicles are equipped with HEV powertrain, the energy consumptions of HEVs are dependent on both vehicle dynamics and powertrain operation. The co-optimization of vehicle dynamics and powertrain operation can make energy consumption reduced further. A decentralized optimization framework aiming to energy efficiency improvement and traveling time minimization is proposed in this paper. In detail, the mathematical optimization problem can be written as follows:

$$\min_{u} \int_{0}^{L} \frac{1}{v_i} \left\{ \lambda * 1 + \left(\frac{\gamma_f}{\rho_f} \dot{m}_f + \gamma_e \dot{m}_e \right) \right\} ds \tag{1}$$

where u is the control input. $\dot{m}_f(g/s)$ and $\dot{m}_e(kWh/s)$ denote the consumption rates of fuel and electricity, respectively. $\gamma_f(¥/L)$ and $\gamma_e(¥/kWh)$ represent the prices of fuel and electricity, respectively. $\rho_f(L/g)$ is the mass conversion rate. s is the sampling distance and λ is the weight factor. In the cost function, the first item concerns about the traveling time and the second item includes both fuel consumption and electricity consumption. It is noted that since the cost function is integrated from 0 to L in space domain, the original function in time domain should be divided by v_i and when vehicle arrives at the origin, v_i is larger than zero. There are constraints, including dynamic-model, inequality constraints of state variables and control inputs, which Eq. (1) has to follow. The detail of these physical constraints will be given in the next section.

3. MODELING

The powertrain structure of parallel HEV is depicted in Fig. 2, the inertias is ignored and vehicle speed v_i dynamics is described as follows:

$$m \frac{dv_i}{dt} = \frac{\tau_{drive,i}}{R_{tire}} - (mg\mu \cos\theta + 0.5\rho A C_d v_i^2) \tag{2}$$

where m, R_{tire}, g, μ, θ, ρ, C_d, A represent vehicle mass, tire radius, gravitational acceleration, rolling coefficient, slop, air density, drag coefficient, and frontal area, respectively. The driving torque $\tau_{drive,i}$ in HEV mode can be determined by the sum of engine torque $\tau_{e,i}$ and motor torque $\tau_{m,i}$.

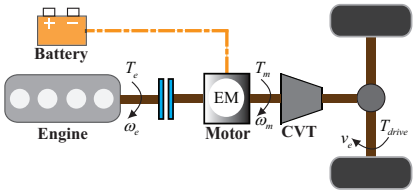

Fig. 2. Structure of parallel HEV.

$$\tau_{drive,i} = i_g i_0 \eta_f (\tau_{e,i} + \tau_{m,i}) \tag{3}$$

where i_g, i_0, η_f represent transmission ratio, differential ratio and transmission efficiency.

Similarly, with determination of i_g and v_i, the engine speed and motor speed in HEV mode can be calculated as follows:

$$\omega_{e,i} = \omega_{m,i} = i_g i_0 \frac{v_i}{R_w} \tag{4}$$

The acceleration a_i is also calculated in following equation:

$$a_i = \frac{dv_i}{dt} = \frac{v_i - v_{i_0}}{t_s} \tag{5}$$

where v_{i_0} and v_i are the current speed and next step speed of vehicle, and t_s is the sampling time. Moreover, the demand vehicle power is calculated as follows:

$$P_{d,i} = v_i \left(\mu mg + 0.5\rho C_D A v_i^2 + m(\frac{v_i - v_{i_0}}{t_s}) \right) \tag{6}$$

In this paper, fuel consumption rate of engine is seen as a nonlinear function of $\tau_{e,i}$ and engine speed $N_{e,i}(rpm)$ in the following equation:

$$\begin{aligned} \frac{dm_{f,i}}{dt} &= a_0 + a_1 N_{e,i} + a_2 N_{e,i}^2 + a_3 N_{e,i}^3 \\ &\quad + a_4 N_{e,i} \tau_{e,i} + a_5 N_{e,i}^2 \tau_{e,i}^2 \end{aligned} \tag{7}$$

where $a_j (j = 0, 1, ..., 5)$ are the identified parameters.

The electricity consumption rate $\dot{m}_e$ is seen as the motor power in this paper, which is determined as follows:

$$\frac{dm_{e,i}}{dt} = P_{b,i} = \frac{\eta_{e,i}(\tau_{m,i}, \omega_{m,i}) \tau_{m,i} \omega_{m,i}}{1000 \times 3600} \tag{8}$$

where $\eta_{e,i}$ demotes the efficiency of motor, which is dependent on $\tau_{m,i}$ and $\omega_{m,i}$.

The distance headway x_i between vehicle i and its preceding vehicle i, p is critical when optimization of vehicle dynamics is considered. The dynamics of x_i is described as follows:

$$\frac{dx_i}{dt} = v_{p,i} - v_i \tag{9}$$

where $v_{p,i}$ is speed of preceding vehicle. Moreover, to ensure the driving safety of vehicle i, the distance headway x_i should satisfy following inequality constraint:

$$x_i \geq x_{i,min} + h * v_i \tag{10}$$

where h and $x_{i,min}$ denote the time headway and minimization of x_i, respectively.

During the transformation from time domain to space domain, the dynamic function of x_i is converted as:

$$\frac{dx_i}{ds} = \frac{dx_i}{dt}\frac{dt}{ds} = \frac{dx_i}{dt}\frac{1}{v_i} = \frac{v_{p,i} - v_i}{v_i} \tag{11}$$

where the vehicle speed v_i should satisfy the speed limit in the merging lane and main lane:

$$0 < v_{i,min} \leq v_i \leq v_{i,max} \tag{12}$$

4. DECENTRALIZED OPTIMIZATION

With modeling information including dynamics-constraint and inequality constraint in above section, the detail optimization problem in Eq. (1) is summarized as follows:

$$\min_{[v_i^*, \tau_{e,i}]^T} \int_{0}^{L} \frac{1}{v_i^*} \left\{ \lambda * 1 + \left(\frac{\gamma_f}{\rho_f} \dot{m}_f + \gamma_e \dot{m}_e \right) \right\} ds \tag{13}$$

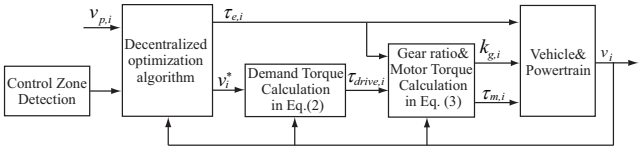

Fig. 3. Block diagram of the optimization design problem.

$$\text{s.t.}\begin{cases} \dfrac{dx_i}{ds} = \dfrac{v_{i,p} - v_i^*}{v_i^*} \\ x_i \geq x_{i,min} + h * v_i^* \\ x_i(0) = x_{i,0} \\ v_{i,min} \leq v_i^* \leq v_{i,max} \\ \tau_{e,min} \leq \tau_{e,i} \leq \tau_{e,max} \\ |\Delta v_i^*| \leq \delta v_i \end{cases}$$

where control inputs are selected as v_i^* and $\tau_{e,i}$, the reason is that v_i^* and $\tau_{e,i}$ are used to optimize vehicle dynamics and powertrain operation, respectively. Moreover, Δv_i^* denotes the variation of vehicle speed, which should be less than the limitation δv_i because there is limitation of maximum power provided by engine and motor.

The block diagram of decentralized optimization design problem is depicted in Fig. 3 and this algorithm can be activated only when vehicle i arrives and enters the control zone. With determination of v_i^*, $\tau_{drive,i}$ can be obtained through Eq. (2) and (5). Then $\tau_{m,i}$ can be determined through Eq. (3) when gear ratio $k_{g,i}$ is given. It is noted that gear ratio $i_{g,i}$ is determined through a rule-based control scheme in this paper, which is a relationship with vehicle speed v_i, fitted as a quadratic function of speed:

$$k_g = c_0 + c_1 v_i^* + c_2 (v_i^*)^2 \tag{14}$$

4.1 PMP-base optimal conditions

Pontryagin's maximum principle (PMP) is employed to solve the constrained optimization problem in Eq. (13). Based on PMP, The Hamiltonian function is written as:

$$H = \frac{1}{v_i^*}\left\{\lambda * 1 + \left(\frac{\gamma_f}{\rho_f}\dot{m}_f + \gamma_e \dot{m}_e\right)\right\} + \frac{(v_{p,i} - v_i^*)}{v_i^*} p \tag{15}$$

where p is the costate to deal with the dynamic-constraint x_i in Eq. (13).

Since there are mixed inequality constraints, including inequality constraints of v_i^* and $\tau_{e,i}$, and mixed inequality constraint between x_i and v_i^*, a Lagrangian function is employed with the multipliers $\lambda_{11}, \lambda_{11}, \lambda_{21}$ and λ_{22}, which is written as follows:

$$\begin{aligned} L = H &+ \lambda_{11}(v_i^* - v_{i,min}) + \lambda_{12}(-v_i^* + w_v) \\ &+ \lambda_{21}(\tau_{e,i} - \tau_{e,i,min}) + \lambda_{22}(-\tau_{e,i} + \tau_{e,i,max}) \end{aligned} \tag{16}$$

where w_v is written as follows:

$$w_v = \min\left\{v_{i,max}, \frac{x_i - x_{i,min}}{h}\right\} \tag{17}$$

Then the costate function is determined as follows:

$$\frac{dp}{ds} = -\frac{\partial L}{\partial x_i} \tag{18}$$

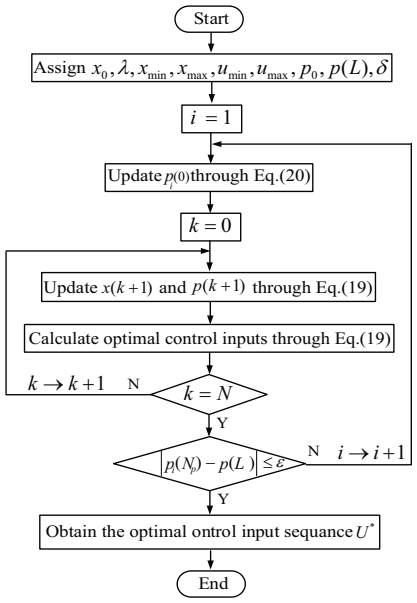

Fig. 4. The flowchart of numerical solution of optimal conditions based on PMP.

In summary the optimal control inputs $u^* = [v_i^*, \tau_{i,e}]$ should satisfy following conditions:

$$\begin{cases} \dfrac{\partial L}{\partial u^*} = 0 \\ H(x, u^*, p, t) \leq H(x, u^*, p, t) \\ \dfrac{dx_i}{ds} = \dfrac{v_{p,i} - v_i^*}{v_i^*} \\ \dfrac{dp}{ds} = -\dfrac{\partial L}{\partial x_i} \\ \lambda_{11} \geq 0, \lambda_{11}(v_i^* - v_{i,min}) = 0 \\ \lambda_{12} \geq 0, \lambda_{12}(-v_i^* + \omega_v) = 0 \\ \lambda_{21} \geq 0, \lambda_{21}(\tau_{e,i} - \tau_{e,i,min}) = 0 \\ \lambda_{22} \geq 0, \lambda_{22}(-\tau_{e,i} + \tau_{e,i,max}) = 0 \\ x_i(0) = x_0 \\ p(L) = 0 \end{cases} \tag{19}$$

where since there is no terminal cost in Eq. (13), terminal costate $p(L)$ is set as zero.

4.2 Numerical solution

The optimal control inputs $u^* = [v_i^*, \tau_{e,i}]^T$ satisfying optimal conditions in Eq. (19) is hard to obtain analytically, a Newton-Raphson method is employed in this paper. The main work is to search an initial costate satisfying terminal costate condition, then the optimal control inputs can be determined through Eq. (19) step by step. The detail mathematical algorithm is shown as follows:

$$p_i(0) = \begin{cases} p_0 & , i = 1 \\ p_1 + \delta & , i = 2 \\ p_{i-1} - \dfrac{\Delta\lambda}{\Delta p}\left(p_i(N_p) - p(L)\right), & i = 3, 4, ... \end{cases} \tag{20}$$

where N_p is the total steps of length L based on sampling length s, δ is the initial parameter, $\Delta\lambda$ and Δp are determined as follows:

$$\begin{cases} \Delta\lambda = p_{i-1}(0) - p_{i-2}(0) \\ \Delta p = p_{i-1}(N_p) - p_{i-2}(N_p) \end{cases} \tag{21}$$

The flowchart of numerical method is depicted in Fig. 4. In the flowchart, ϵ is the tolerance factor.

5. SIMULATION RESULTS

Table 1. Parameters of the parallel HEV

Parameters	Symbol	Values
Vehicle mass	M	1138[kg]
Wheel radius	R_w	0.3015[m]
Air density	ρ_{air}	1.2[kg/m^3]
Front area	A	2.239[m^2]
Drag coefficient	C_d	0.32
Rolling resistance	μ	0.022
Differential efficiency	η_f	0.98
Final differential ratio	i_0	3.95
Maximum gear ratio	$i_{g,max}$	3.5
Minimum gear ratio	$i_{g,min}$	0.65

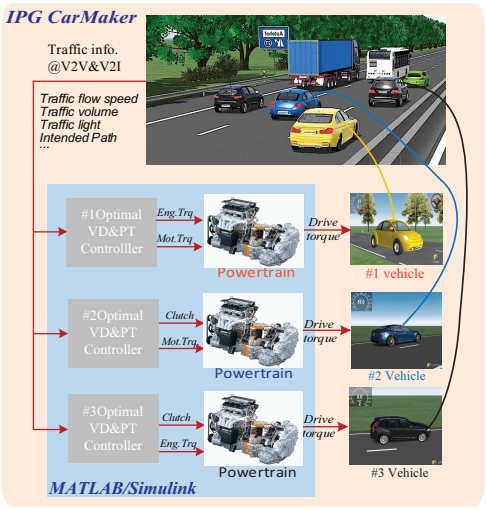

Fig. 5. The structure of multi-vehicle-controllable traffic-in-the-loop powertrain simulator.

The simulation are conducted on a multi-vehicle-controllable traffic-in-the-loop powertrain simulator, depicted in Fig. 5. The parameters of HEVs is listed in Table. 1. Because of the page limitation, only a case study is given in this extended abstract. A traffic scenario that is shown in Fig.1 with three vehicles is generated in the simulator and the simulation results are shown in Fig. 6. It is seen that the speeds of three vehicles are finally identical and the headway distances are within the limitations. Moreover, the results under different electricity prices $\gamma_{e1} < \gamma_{e2} < \gamma_{e3}$ and weight factors $\lambda_1 < \lambda_2 < \lambda_3$ are shown in Table. 2. It can be concluded that when electricity price is low enough, all power is provided by the motor ; however, motor may even work in generation mode when the electricity is high enough. On the other hand, the λ can influence the traveling time and the monetary consumption. Higher λ means less time and more monetary cost.

6. CONCLUSION

In this paper, the problem of optimal coordination of HEVs at merging roadways with consideration of powertrain operation is addressed. A decentralized optimal control framework is proposed to improve fast past and

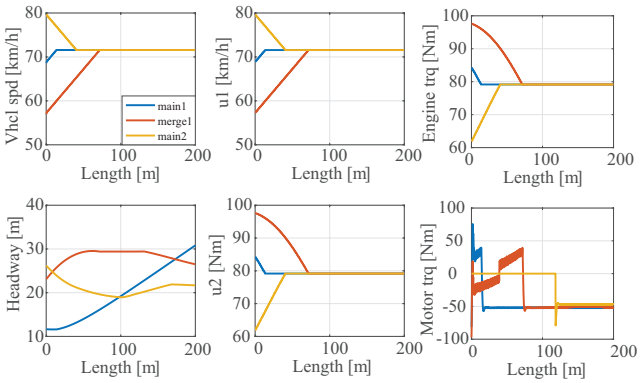

Fig. 6. Consumptions of engine and battery and total consumption in monetary sense.

Table 2. Performance comparison over different electricity prices r_e and weight factors λ

Vhcl	Case	Fuel[g]	Ele[kWh]	Case	Cost[¥]	Tim[s]
#i	γ_{e1}	0	0.059	λ_1	1.34	11.59
	γ_{e2}	13.6	-0.001	λ_2	1.67	11.03
	γ_{e3}	30.3	-0.062	λ_3	2.21	10.37
#i-1	γ_{e1}	0	0.073	λ_1	2.00	13.36
	γ_{e2}	15.9	-0.003	λ_2	2.32	12.99
	γ_{e3}	32.2	-0.054	λ_3	2.84	12.58
#i-2	γ_{e1}	0	0.027	λ_1	1.60	14.91
	γ_{e2}	12.0	-0.021	λ_2	2.10	14.67
	γ_{e3}	29.4	-0.089	λ_3	2.56	14.06

energy utilization efficiency. The simulation validations show the effectiveness of the proposed algorithm in a simulator with combination of commercial traffic simulator and enterprise-level powertrain modeling.

REFERENCES

J. Guanetti, Y. Kim and F. Borrelli. *Control of Connected and Automated Vehicles: State of the Art and Future Challenges. Annual Reviews in Control*, 45:18–40, 2018.

J. Rios-Torres, A. A. Malikopoulos. *Automated and Cooperative Vehicle Merging at Highway On-Ramps. IEEE Transactions on Intelligent Transportation Systems*, 18(4):780–789, 2017.

W. Cao, M. Mukai, T. Kawabe, H. Nishira. *Cooperative Vehicle Path Generation During Merging Using Model Predictive Control with Real-time Optimization. Control Engineering Practice*, 34:98–105, 2015.

W. Xiao, C. G. Cassandras. *Decentralized Optimal Merging Control for Connected and Automated Vehicles. American Control Conference*, Philadelphia, USA, July 10-12, 3315–3320, 2019.

Y. Ito, M. A. S. Kamal, T. Yoshimura. *Coordination of Connected Vehicles on Merging Roads Using Pseudo-Perturbation-Based Broadcast Control. IEEE Transactions on Intelligent Transportation Systems*, 20(9):3496–3512, 2019.

Z. Zhao, Z. Wang, G. Wu, F. Ye, M. J. Barth. *The State-of-the-Art of Coordinated Ramp Control with Mixed Traffic Conditions. arXiv preprint*, arXiv:1908.00573, 2019.